MATEMATIKA, MJIAM, Volume 42, Number 1, 1–11

Effects of Skin Thermoregulation Delay in a Dynamical Model of Heat Transfer in an Infant Incubator

Kenneth Ivan B. Ramos*, Alfred Devon D. Tolentino and Juancho A. Collera

Department of Mathematics and Computer Science, University of the Philippines Baguio, Governor Pack Road, Baguio City 2600, Philippines.

*Corresponding author: kbramos7@up.edu.ph

Article history
Received: 9 February 2025
Received in revised form: 25 August 2025
Accepted: 18 September 2025
Published on line: 1 April 2026

Abstract Infant incubators are lifelines for millions of premature and sick infants worldwide. This device regulates an appropriate environment, where temperature control holds utmost importance. Heat transfer in infant incubators was previously studied using ODE models that did not account for temperature fluctuations due to fat and skin thickness. Hence, a system of delay differential equations describing heat transfer in an infant incubator considering skin thermoregulation delay, which is reflected using a time-delay parameter, is proposed and analyzed in this paper. Initial results include the existence of a unique positive equilibrium describing the ideal temperatures of the infant's core, skin, and the incubator's air space. To investigate the effects of the skin thermoregulation delay on the dynamical behavior near the equilibrium, a local stability analysis was performed using the time delay as the main parameter. Conditions for the absolute stability of the equilibrium and occurrence of stability switches were derived. In the latter case, a locally asymptotically stable equilibrium can become unstable due to the occurrence of a Hopf bifurcation at a threshold value of the time-delay parameter. Numerical simulations reveal that the limit-cycle solutions born from the Hopf bifurcation can lead to extreme temperature fluctuations, catastrophic for the infant. To maintain the ideal temperatures, the aim is to have conditions where the equilibrium is either absolutely stable or the time-delay parameter is kept lower than the threshold value. This paper helps to better understand the dynamics of heat transfer in an infant incubator, which benefits premature and sick infants.

Keywords Infant incubator, core temperature, skin temperature, airspace temperature, skin thermoregulation delay, equilibrium, limit-cycle solutions.

Mathematics Subject Classification 34K13, 37G10.

1 Introduction

As of the year 2024, there are about 4.3 humans born every second worldwide [1]. Infants born before the end of the three-trimester period, referred to as premature or preterm babies,

are typically born three weeks before their due date [2]. However, any infant delivered earlier than the calculated due date is considered *premature*. Preterm infants are physically vulnerable since they are underdeveloped and unable to survive on their own [3]. According to the World Health Organization in 2023, over the past decade, nearly 1 in 10 infants around the world has been born prematurely. Moreover, preterm birth complications have been the leading cause of death in children of ages 5 years and below worldwide [4].

For premature babies to grow and develop properly, different medical procedures are done, including keeping them in a controlled hygrothermal environment. The amount of medical care that a premature infant needs depends on its gestational age, ranging from late preterm to extremely preterm; that is, the earlier a neonate is born, the greater care it requires [2, 3]. Preterm infants require medical intervention for functions they cannot manage on their own, which often results in their immediate admission to the Neonatal Intensive Care Unit (NICU). In this unit, premature neonates are helped with their feeding, breathing, gaining weight, and maintaining body temperature [2], and are kept in an incubator.

An *infant incubator* is a medical device shaped like a box with transparent sections and various controls that regulates an environment needed for an infant's growth and survival. It is typically catered for the sick and premature babies. Incubators were invented to aid the thermoregulation of newborns. The underdeveloped brain of a neonate usually struggles to regulate body temperature effectively [5]. It relies on detecting elevated heat dissipation through the skin and responding to it. However, the capacity of premature infants to minimize water loss and enhance skin insulation is restricted and often insufficient. Despite an infant's attempts to generate internal heat using its own energy, it gradually cools down to temperatures around 30°C or even lower. By simply supplying external heat, the infant can be maintained at a normal body temperature and survive.

Skin thickness is a genetic trait [6] that largely affects thermal conductivity and threshold [7]. The thermal conductivity of the skin correlates to skin thickness; that is, the thinner the skin, the higher its conductivity [7]. The composition of soft tissue in infants, such as the skin, varies so differently from adults [8]. Hence, there are more things to consider in terms of the skin's temperature regulation for an infant. Thermal conductivity of the skin varies largely, which in turn affects temperature regulation [9]. The outer layer of the skin, the *epidermis*, varies throughout the body [10]. The eyelids and the genitalia have the thinnest skin [10]. The next layer of the skin, the *dermis*, also varies in thickness. *Subcutaneous fat*, also a part of the skin, also largely affects the heat transfer since it holds utmost importance in temperature maintenance [10, 11]. The fat content of the human skin differs greatly in different parts of the body [12]. In turn, the body processes temperature through the subcutaneous fat differently [10–12]. Especially compared to full-term, premature infants have more fat content, resulting in differences in regulation of temperature through the subcutaneous layer of the skin [13]. Therefore, there's a considerable time delay in skin thermoregulation, an important mechanism in the infant incubator system, as infants placed in the devices need to attain certain bodily temperatures to grow. Skin temperature is a variable that responds less quickly in thermoregulation, implying that skin temperature brings in a delay in the response time of the system [14–16]. Ultimately, it is observed that skin temperature does involve time delay in thermoregulation-referred to here as *skin thermoregulation delay*.

The present paper studies a generalization of the earlier ODE model of Simon *et al.* [16] to include this time delay in thermoregulation due to fat and skin thickness. To the best of our

knowledge, this is the first delay differential equations (DDEs) model in this topic. The goal of this paper is to examine how the skin thermoregulation delay influences the infant temperatures. Thus, obtaining insights and strategies that would help premature and sick infants.

In the following section, the details of the proposed model and the ideal temperatures of the system are given. Then in the main results section, the effects of varying the skin thermoregulation delay are examined, both theoretically and numerically. The paper concludes with a summary and future directions of this research work.

2 The Proposed Model

In 1994, Simon *et al.* [16] established a spatially lumped theoretical model of heat transfer in an infant incubator system which includes five compartments; namely, the infant's core, skin, the incubator air space, wall, and mattress. Following their model and to account for skin thermoregulation delay, a time delay within the skin compartment was introduced. This results to the following proposed dynamical model of heat transfer in an infant incubator with skin thermoregulation delay

$$\begin{cases} \frac{d}{dt}x(t) &= p_1 - p_2x(t) + p_2y(t) + p_3z(t), \\ \frac{d}{dt}y(t) &= p_4 + p_5x(t) - p_6\left(y(t) + 273.15\right)^4 + p_7z(t) - p_8y(t-\tau), \\ \frac{d}{dt}z(t) &= p_9 + p_{10}y(t) - p_{11}z(t), \end{cases} \tag{1}$$

where $x(t), y(t)$ and $z(t)$ denote, respectively, the temperatures of the infant's core, the infant's skin, and the incubator airspace, all in degree Celsius. The parameters $\{p_i\}_{i=1}^{11}$ are a combination of infant-specific and incubator-specific parameters and all are positive real numbers. The number 273.15 in the second equation of the above system accounts for temperature conversion since the original ODE model in Simon *et al.* [16] is in Kelvin scale. It is also worth noting that the special case when $\tau = 0$ in the system Eq. (1) yields the reduced ODE model studied in Simon *et al.* [16]. In other words, one can view the DDE model in the system Eq. (1) as a generalization of the previous ODE model. Table 1 provides the description of the model parameters, as well as their approximate values based on the previous work of Simon *et al.* [16]. This same set of parameter values will be used later on in the numerical simulation in order to compare the dynamics of the original ODE model to dynamics of the proposed DDE model given in the system Eq. (1).

2.1 Ideal Temperatures

An equilibrium $E_* = (x_*, y_*, z_*)$ of the system Eq. (1) can be obtained by solving simultaneously the equations $\frac{d}{dt}x(t) = 0$, $\frac{d}{dt}y(t) = 0$ and $\frac{d}{dt}z(t) = 0$. That is, the equilibria of the system Eq. (1) are constant through time. Moreover, since the proposed system has no delay-dependent coefficients, $y(t)$ can be used instead of $y(t-\tau)$ in solving for the equilibrium.

Solving for the equilibrium, the components x_*, y_* and z_* must satisfy the following system of equations

$$p_1 - p_2x + p_2y + p_3z = 0, \tag{2}$$

$$p_4 + p_5x - p_6\left(y + k\right)^4 + p_7z - p_8y = 0, \tag{3}$$

$$p_9 + p_{10}y - p_{11}z = 0, \tag{4}$$

Table 1: Description of system parameters and their approximate values

Parameter	Description	Approximate Value	Unit
p_1	heat production by metabolic activity	4.44×10^{-4}	$^\circ C/_s$
p_2	core thermoregulation constant	2.00×10^{-4}	$1/_s$
p_3	heat transfer through breathing	5.30×10^{-7}	$1/_s$
p_4	effects of environmental condition to the skin	1.23×10^{-1}	$^\circ C/_s$
p_5	heat transfer through blood in infant's skin	1.50×10^{-6}	$1/_s$
p_6	effects of the incubator walls to the skin	5.03×10^{-12}	$^\circ C/(K^4 s)$
p_7	heat transfer on skin exposed to air	3.66×10^{-4}	$1/_s$
p_8	skin thermoregulation constant	2.57×10^{-3}	$1/_s$
p_9	overall climate of air	3.74×10^{-1}	$^\circ C/_s$
p_{10}	condition of the air exposed to the skin	2.25×10^{-3}	$1/_s$
p_{11}	air thermoregulation constant	1.47×10^{-2}	$1/_s$
τ	skin thermoregulation delay	> 0 (varies)	s

where, for the sake of brevity, the number 273.15 is replaced with k. From the equation Eq. (4), the following expression for z in terms of y is obtained

$$z \quad = \quad \frac{p_9 + p_{10}y}{p_{11}}. \tag{5}$$

Meanwhile, using the equations Eq. (2) and Eq. (5), the following expression for x in terms of y is derived

$$x \quad = \quad \frac{(p_1p_{11} + p_3p_9) + (p_2p_{11} + p_3p_{10})y}{p_1p_{11}}. \tag{6}$$

Plugging in the expressions for x and z given, respectively, in equations Eq. (6) and Eq. (5) to the equation Eq. (3), the following degree-four polynomial equation in y can be obtained

$$R(y) \quad := \quad r_4y^4 + r_3y^3 + r_2y^2 + r_1y + r_0 \quad = \quad 0 \tag{7}$$

where $r_0 = p_5(p_1p_{11}+p_3p_9)/p_2p_{11}+p_7p_9/p_{11}+p_4-k^4p_6$, $r_1 = p_5(p_3p_{10}+p_2p_{11})/p_2p_{11}+p_7p_{10}/p_{11}-p_8-4k^3p_6$, $r_2 = -6k^2p_6$, $r_3 = -4kp_6$, and $r_4 = -p_6$. If the polynomial R satisfies the following conditions

$$r_0 > 0 \qquad \text{and} \qquad R'(y) < 0 \text{ for all } y > 0, \tag{8}$$

then the equation Eq. (7) has a unique positive root, which will be denoted by y_+. This positive value y_+ then yields the positive values x_+ and z_+ using the equations Eq. (6) and Eq. (5), respectively, since all the p_i's are positive. For the set of parameter values listed in Table 1, one can easily verify that the conditions on Eq. (8) are both satisfied and the unique positive root of the quartic polynomial equation Eq. (7) is $y_+ \approx 34.685318$. Consequently, the positive values $x_+ \approx 36.986809$ and $z_+ \approx 30.751154$ are obtained from equations Eq. (6) and Eq. (5), respectively. From now on, the temperature values given by the components of *the positive equilibrium*

$$E_+ \quad := \quad (x_+, y_+, z_+) \quad \approx \quad (36.986809, 34.685318, 30.751154) \tag{9}$$

will be referred to as *ideal temperatures*. Figure 1 shows the time-series plot of the temperatures when $\tau = 0$ (left panel) and when $\tau = 500$ (right panel). The equilibrium E_+, as given in the equation Eq. (9), is locally asymptotically stable for both cases. Although, for the case with $\tau = 500$, the solutions tend to oscillate first before settling to the ideal temperature values.

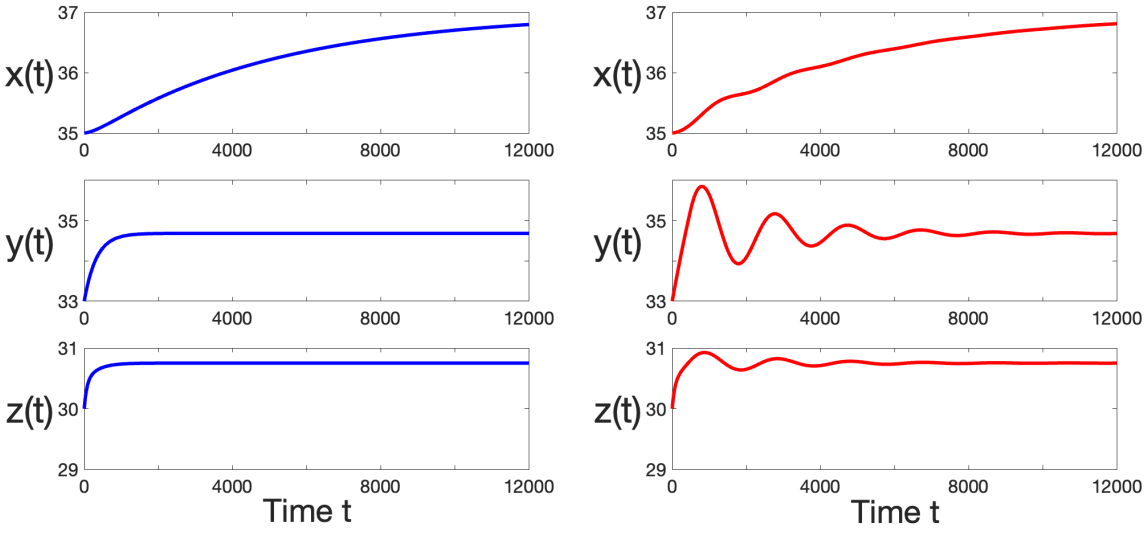

Figure 1: Time-series plot of the temperatures when $\tau = 0$ (left) and when $\tau = 500$ (right), both using the parameter values in Table 1 and the initial history $(x(t), y(t), z(t)) = (35, 33, 30)$ for $t \in [-\tau, 0]$.

The dynamics near the positive equilibrium E_+ of the system Eq. (1) can be determined by analyzing the characteristic equation corresponding to the linearized system about E_+. For $\tau \geq 0$, this equation is given by the following transcendental equation

$$\left(\lambda^3 + a_1\lambda^2 + a_2\lambda + a_3\right) + \left(a_4\lambda^2 + a_5\lambda + a_6\right) e^{-\lambda\tau} \quad = \quad 0, \tag{10}$$

where $a_1 = p_2 + p_{11} + 4p_6(k + y_+)^3$, $a_2 = p_2p_{11} - p_2p_5 - p_7p_{10} + 4p_6(p_2 + p_{11})(k + y_+)^3$, $a_3 = 4p_2p_6p_{11}(k+y_+)^3 - p_3p_5p_{10} - p_2p_7p_{10} - p_2p_5p_{11}$, $a_4 = p_8$, $a_5 = p_2p_8 + p_8p_{11}$, and $a_6 = p_2p_8p_{11}$. If all roots of the characteristic equation Eq. (10) lie in the open left-half of the complex plane, then the positive equilibrium E_+ is locally asymptotically stable (LAS) [17].

In the section that follows, the sufficient conditions for E_+ to be LAS will be derived. Also, the authors examine the possibility of stability switches. In particular, the scenario where a LAS E_+ becomes unstable due to the occurrence of a Hopf bifurcation in the system Eq. (1).

3 Main Results

When $\tau = 0$, the characteristic equation Eq. (10) reduces to the following cubic equation

$$\lambda^3 + (a_1 + a_4)\lambda^2 + (a_2 + a_5)\lambda + (a_3 + a_6) \quad = \quad 0. \tag{11}$$

By the well-known Routh-Hurwitz criterion, all the roots of the cubic equation Eq. (11) lie in the open left-half of the complex plane provided the following conditions

$$(a_1 + a_4) > 0, \quad (a_2 + a_5) > 0, \quad (a_3 + a_6) > 0, \quad \text{and} \quad (a_1 + a_4)(a_2 + a_5) > (a_3 + a_6) \tag{12}$$

hold. Consequently, the following result is obtained.

Theorem 1 *The equilibrium E_+ of the system* (1) *with $\tau = 0$ is LAS if the inequalities in Eq. (12) are all satisfied.*

Theorem 1 means that at $\tau = 0$, all roots of the characteristic equation Eq. (10) are inside the open left-half of the complex plane provided that the conditions on Eq. (12) are all satisfied. Since the roots λ of the equation Eq. (10) depends on τ, increasing τ may cause the roots to cross the imaginary axis and move towards the open right-half of the complex plane. When this happens, the equilibrium E_+ becomes unstable. In contrast, if all the roots remain in the open left-half of the complex plane, then E_+ remains LAS. This latter case is referred to in the literature as absolute stability, in which a LAS equilibrium remains LAS for all $\tau > 0$ [18].

3.1 Absolute Stability of the Positive Equilibrium

In the following, the conditions that guarantee the absolute stability of E_+ is derived. First, notice that $\lambda = 0$ is not a root of the characteristic equation Eq. (10) since $(a_3 + a_6) > 0$ from the conditions on Eq. (12). This means that the roots of the characteristic equation Eq. (10) cannot cross the imaginary axis through the origin. Suppose now that $\lambda = i\omega$, with $\omega > 0$, is a root of the characteristic equation Eq. (10). Then, $(-i\omega^3 - a_1\omega^2 + ia_2\omega + a_3) + (a_4\omega^2 + ia_5\omega + a_6)(\cos\omega\tau - i\sin\omega\tau) = 0$. Separating the real and imaginary parts, gives

$$(a_4\omega^2 - a_6)\cdot\cos(\omega\tau) \quad - \quad a_5\omega\cdot\sin(\omega\tau) \quad = \quad -a_1\omega^2 + a_3, \tag{13}$$

$$(a_4\omega^2 - a_6)\cdot\sin(\omega\tau) \quad + \quad a_5\omega\cdot(\cos\omega\tau) \quad = \quad \omega^3 - a_2\omega. \tag{14}$$

Now, eliminating τ, yields $(a_4\omega^2 - a_6)^2 + (a_5\omega)^2 = (-a_1\omega^2 + a_3)^2 + (\omega^3 - a_2\omega)^2$. This gives an even polynomial in ω of degree six which, after letting $\mu = \omega^2$, can be further reduced into the following cubic polynomial in u

$$h(\mu) \quad := \quad \mu^3 + b_2\mu^2 + b_1\mu + b_0 \quad = \quad 0 \tag{15}$$

where $b_2 = a_1^2 - a_4^2 - 2a_2$, $b_1 = a_2^2 - 2a_1a_3 + 2a_4a_6 - a_5^2$ and $b_0 = a_3^2 - a_6^2$. If h has no positive root, then the characteristic equation Eq. (10) cannot have purely imaginary roots, i.e. $\lambda = i\omega$ is not a root of the equation Eq. (10). In other words, the roots of the characteristic equation Eq. (10) remain in the open left-half of the complex plane for all $\tau > 0$. The following result summarizes the above discussion.

Theorem 2 *Suppose that the conditions on Eq.* (12) *are all satisfied, and the cubic equation Eq.* (15) *does not have any positive roots. Then, the positive equilibrium E_+ of the system Eq.* (1) *is absolutely stable, i.e. E_+ is LAS for all $\tau > 0$.*

3.2 Hopf Bifurcation at the Positive Equilibrium

As illustrated in Fig. 1, increasing the value of τ causes the temperatures to fluctuate. However, under the conditions of Theorem 2, these temperatures will eventually settle to the ideal temperatures. The possibility of sustained temperature oscillations in the model is now considered. The authors claim that this occurs due to a Hopf bifurcation when τ reaches a certain

threshold value and the equilibrium E_+ becomes unstable. In contrast to Theorem 2, it is now assumed that the cubic equation Eq. (15) has at least one positive root.

Suppose that the characteristic equation Eq. (10) has a pair of purely imaginary simple roots $\lambda = \pm i\omega_+$. Here, $\omega_+ = \sqrt{u_+}$ where u_+ is a simple positive root of the cubic equation Eq. (15). The root λ can be viewed as a smooth function of τ, and at some critical values $\tau = \tau_k$, the roots $\lambda(\tau_k)$ lie on the imaginary axis. To compute the critical values τ_k, one can solve for $\cos(\omega\tau)$ and $\sin(\omega\tau)$ from the equations Eq. (13) and Eq. (14). Then, using the expression for $\cos(\omega\tau)$, yields the values

$$\tau_k \;=\; \frac{1}{\omega_+}\cdot\cos^{-1}\left(\frac{a_5\omega_+^2(\omega_+^2-a_2)-(a_4\omega_+^3-a_6)(a_1\omega_+^2-a_3)}{a_4^2\omega_+^4+(a_5^2-2a_4a_6)\omega_+^2+a_6^2}+2\pi k\right), \qquad k=0,1,2,\ldots. \tag{16}$$

To determine if and how the roots λ of the characteristic equation (10) will traverse the imaginary axis, the following relationship derived in [19] can be used

$$\operatorname{sign}\left\{\frac{d}{d\tau}\mathrm{Re}\;\lambda(\tau)\bigg|_{\tau\,=\,\tau_k}\right\} \;=\; \operatorname{sign}\left\{h'(u_+)\right\}. \tag{17}$$

If $h'(u_+) > 0$ (respectively, $h'(u_+) < 0$), then the roots of the characteristic equation Eq. (10) that are on the imaginary axis at $\tau = \tau_k$ will move towards the open right-half (respectively, towards the open left-half) of the complex plane. The following theorem formally states the main result of this paper. Its proof follows from the Hopf bifurcation theorem [17].

Theorem 3 *Suppose that the conditions on Eq.* (12) *are all satisfied, and the cubic equation Eq.* (15) *has a simple positive root* u_+ *with* $h'(u_+) > 0$. *Denote by* $\tau^* = \min\{\tau_k \mid \tau_k > 0\}$. *Then, the positive equilibrium* E_+ *of the system Eq.* (1) *is locally asymptotically stable when* $\tau \in (0, \tau^*)$. *Moreover, when* $\tau = \tau^*$, *the system Eq.* (1) *undergoes a Hopf bifurcation at* E_+, *and the positive equilibrium* E_+ *becomes unstable.*

Now, Theorem 3 is illustrated using the set of parameter values listed in Table 1. At $\tau = 0$, the positive equilibrium E_+ given in the equation Eq. (9) is LAS since the conditions on Eq. (12) are all satisfied, i.e. all roots of the equation Eq. (11) have negative real parts. The cubic equation Eq. (15) has a unique positive root $u_+ \approx 6.274212 \times 10^{-6}$, which gives $\omega_+ \approx 0.002505$. Moreover, the graph of h is increasing at $u = u_+$, i.e. $h'(u_+) > 0$. The sequence $\{\tau_k\}$ is increasing, so $\tau^* = \tau_0 \approx 710.424349$. Theorem 3 guarantees that the positive equilibrium E_+ is LAS when $\tau < \tau^*$. Since, in this case, the cubic equation Eq. (15) has exactly one positive root u_+ with $h'(u_+) > 0$, the equation Eq. (17) tells us that the roots of the characteristic equation Eq. (10) can only traverse the imaginary axis from left to right. Hence, here, E_+ is unstable when $\tau > \tau^*$. This one-time switch towards instability is due to the Hopf bifurcation occurring when $\tau = \tau^*$. Figure 2 shows this stability switch scenario. The left panel shows that E_+ is LAS when $\tau = 650 < \tau^*$. Meanwhile, the right panel shows that E_+ is unstable when $\tau = 711 > \tau^*$ and a stable limit cycle persists in this case.

3.3 Numerical Simulation

The numerical continuation and bifurcation analysis tool for systems of delay differential equations developed by Engelborghs *et al.* [20], called *DDE-BIFTOOL*, allows us to examine the

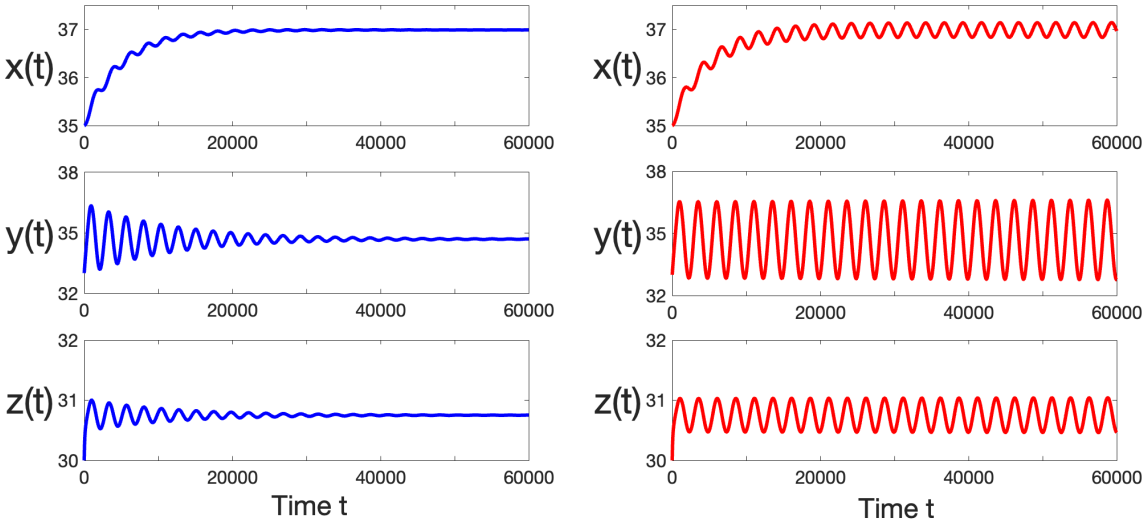

Figure 2: Time-series plot of the temperatures when $\tau = 650$ (left) and when $\tau = 711$ (right) showing the switch towards instability at $\tau = \tau^* \approx 710.424349$ where a Hopf bifurcation occurred.

dynamics of the system Eq. (1) beyond what is guaranteed by Theorem 3. In particular, one can say more about the periodic orbit that is created by the Hopf bifurcation (*e.g.* in terms of its stability and amplitude). Exploring 2-parameter bifurcation diagrams is also possible through this tool, which enables us to determine the effects of changing certain parameters, particularly those that are incubator-related, on the dynamical behavior of the system Eq. (1).

Figure 3 shows the branch of the positive equilibria E_+ (horizontal line), as well as the branch of the limit-cycle solutions (curve) created by the Hopf bifurcation when $\tau = \tau^* \approx 710.424349$. The authors refer the reader to the tutorial in [21] on generating such diagrams. The equilibrium E_+ is LAS for $\tau < \tau^*$ and is unstable for $\tau > \tau^*$. Here, the line color green means LAS while red means unstable. The Hopf bifurcation at $\tau = \tau^*$, marked with an asterisk, is where the stability switch occurred, and where the branch of limit cycles emerges. The Hopf bifurcation is supercritical, *i.e.* the bifurcating limit cycles are stable.

An observation here, based on the diagrams in Fig. 3, is that once $\tau > \tau^*$, the temperatures can deviate further from the ideal temperatures. Such scenario should be avoided in order to maintain temperatures suitable for the infant. Ideally, as illustrated in Fig. 1, the goal is for the temperatures to stay close to the ideal temperatures, or at least settle to the ideal temperatures quicker or in less time.

Next, the effects of varying the values of some incubator-related parameters on the stability of E_+ are examined. In particular, the parameters p_4 which has an inverse relationship to mattress thickness and p_{11} which has a direct relationship to the speed of air flow, are considered. Figure 4 shows the two-parameter diagrams where the Hopf bifurcation curve (blue curve) partitions the parameter space into regions where E_+ is LAS and where it is unstable. The left panel indicates that p_4 should have a higher value to make E_+ LAS. Similarly, the right panel implies that p_{11} should have a lower value to make E_+ LAS.

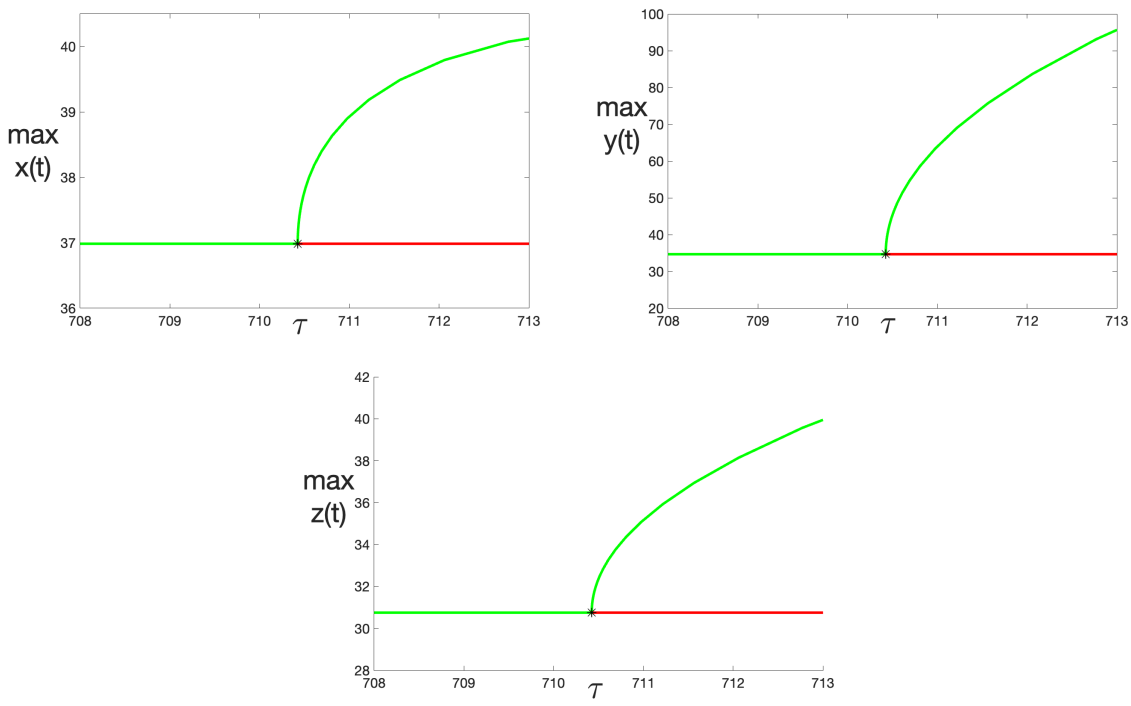

Figure 3: Branch of the positive equilibria E_+ (horizontal line) obtained by varying τ. Stable and unstable parts of the branch are shown in green and red, respectively. The stability switch occurred at a Hopf bifurcation, marked with asterisk, where a stable branch of limit-cycle solutions (green curve) emerges.

4 Summary and Future Directions

Infant incubators are indispensable in helping neonates, particularly premature babies, improve their health. Maintaining the neonate's body temperature ideal is one aspect where an infant incubator is useful. The proposed model describes the heat transfer between the infant's core, skin, and the incubator air space considering the effects of the skin thermoregulation delay that is due to, *e.g.*, the fat and skin thickness of the neonate. The model has a unique positive equilibrium whose components represent the ideal temperatures. For small values of the skin thermoregulation delay, the temperatures fluctuate before settling to the ideal temperatures. However, if its value crosses a certain threshold, sustained oscillations were observed. In the former case, the equilibrium is locally asymptotically stable, while in the latter case the system had undergone a Hopf bifurcation, which gave rise to the periodic behavior of the temperatures around the ideal temperature values. These sustained oscillations can lead to dangerous deviations from the ideal temperatures, and thus must be avoided. Sufficient conditions that guarantee the local asymptotic stability of the equilibrium as well as the conditions for the occurrence of a Hopf bifurcation were established. Hence, one can consider these conditions in order to achieve the ideal temperatures and avoid the case of having temperatures that are way off the ideal values. Furthermore, emphasis has been placed on the strategy of varying the incubator-related parameters, *i.e.* those parameters that can be changed physically, to achieve the above mentioned goals.

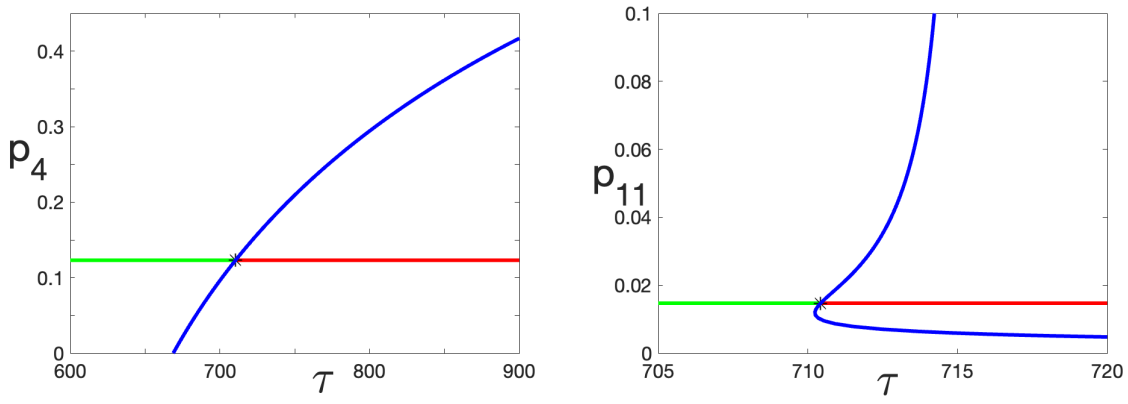

Figure 4: Hopf bifurcation curves (blue) partitioning the parameter space into regions where E_+ is LAS and where it is unstable.

As for future directions of this research, the authors recommend using updated parameter values based on a modern or contemporary infant incubator design if ever it's available. Another recommendation is to explore bifurcations of higher codimension to further examine the effects of varying several parameters simultaneously, and thus gaining better insights in designing the appropriate incubator environment that ultimately benefits the premature and sick infants.

Acknowledgments

The authors thank the reviewers whose comments and suggestions further improved the article. The authors also acknowledge the support of the Department of Mathematics and Computer Science of the University of the Philippines Baguio.

References

[1] People and Society. *The World Factbook. https:// www.cia.gov/ the-world-factbook/ countries/ world/ #people-and-society.* (Accessed 7 June 2024)

[2] Premature Birth: Complications, Management & Causes. *Cleveland Clinic. https:// my.clevelandclinic.org/ health/ diseases/ 21479-premature-birth.* (Accessed 7 June 2024)

[3] Nöcker-Ribaupierre, M. Guidelines for Music Therapy Practice in Pediatric Care. *Premature infants.* 2013. 48. *https://www.researchgate.net/publication/301219860.* (Accessed 7 June 2024)

[4] Preterm birth. World Health Organization. 2023. *https://www.who.int/news-room/clevel-sheets/detail/preterm-birth.* (Accessed 7 June 2024)

[5] Infant Incubator. Sri Ramaswamy Memorial University Institute of Science and Technology. *https://webstor.srmist.edu.in.* (Accessed 7 June 2024)

[6] Fuller, C.K. Understanding Your Skin. *Epiphany Dermatology.* 2024.

[7] Stoll, A.M. Thermal Properties of Human Skin Related TO Nondestructive Measurement of Epidermal Thickness. *Journal of Investigative Dermatology*. 1977. 69(3):328–332. doi=https://doi.org/10.1111/1523-1747.ep12507865

[8] Kultubay, Z. et al. Newborn Skin: Common Skin Problems. *National Library of Medicine*. 2017. *PMC5574071*.

[9] Cohen, M.L. Measurement of the Thermal Properties of Human Skin. A Review. *Journal of Investigative Dermatology*. 1977. 69(3): 333–338. doi=https://doi.org/10.1111/1523-1747.ep12507965

[10] Poonawalla, T. and Diven, D. Anatomy of the Skin. *Core Concepts of Pediatrics*. 2008. *https://www.utmb.edu/pedi_ed/CoreV2/Dermatology/page_03.htm*. (Accessed 7 June 2024)

[11] Speakman, J.R. Obesity and thermoregulation. *National Library of Medicine*. 2018. doi= 10.1016/B978-0-444-63912-7.00026-6

[12] Subcutaneous Fat. *Cleveland Clinic*. 2022. *https://my.clevelandclinic.org/health/diseases /23968-subcutaneous-fat*. (Accessed 7 June 2024)

[13] Hamatschek, C. et al. Fat and Fat-Free Mass of Preterm and Term Infants from Birth to Six Months: A Review of Current Evidence. *National Library of Medicine*. 2022. doi=10.3390/nu12020288

[14] Romanovsky, A.A. Skin temperature: its role in thermoregulation *National Library of Medicine*. 2014. doi=10.1111/apha.12231

[15] Wakim, S. and Grewall, M. Homeostasis and Feedback. *LibreTexts Biology*. (n.d.). *https://bio.libretexts.org/Bookshelves/Human_Biology/Human_Biology_(Wakim_and _Grewal) (Accessed 7 June 2024)*

[16] Simon, B.N. Jr., Reddy, N.P. and Kantak, A. A theoretical model of infant incubator dynamics. *J. Biomech. Eng*. 1994. 116(3):263–269. doi=10.1115/1.2895729

[17] Smith, H.L. An Introduction to Delay Differential Equations with Applications to the Life Sciences. *Springer*. 2010.

[18] Brauer, F. Absolute stability in delay equations. Elsevier. *Journal of Differential Equations*. 1987. 69(2):185–191.

[19] Kuang, Y. Delay Differential Equations with Applications in Population Dynamics. *Academic Press*. 1933.

[20] Engelborghs, K., Luzyanina, T. and Roose, D. Numerical bifurcation analysis of delay differential equations using DDE-BIFTOOL. ACM. *ACM Transactions on Mathematical Software (TOMS)*. 2002. 28(1):1–21.

[21] Collera, J.A. Numerical continuation and bifurcation analysis in a harvested predator-prey model with time delay using DDE-Biftool. Springer. *Dynamical Systems, Bifurcation Analysis and Applications*. 2019. 1–21.